Domain Dynamics in a Ferroelastic Epilayer on a Paraelastic Substrate

Y. F. Gao

Z. Suo

Mechanical and Aerospace Engineering Department and Princeton Materials Institute, Princeton University, Princeton, NJ 08544

This paper models the domain dynamics in a ferroelastic epilayer within the time-dependent Ginzburg-Landau (TDGL) framework. Constrained on a paraelastic substrate of square symmetry, the epilayer has rectangular symmetry, and forms domains of two variants. The domain wall energy drives the domains to coarsen. The spontaneous strains induce an elastic field, which drives the domains to refine. The competition between coarsening and refining selects an equilibrium domain size. We model the epilayer-substrate as a nonequilibrium thermodynamic system, evolving by the changes in the elastic displacements and the order parameters. The free energy consists of two parts: the bulk elastic energy, and the excess surface energy. The elastic energy density is taken to be quadratic in the strains. The surface energy density is expanded into a polynomial of the order parameters, the gradients of the order parameters, and the strains. In this expansion, the surface stress is taken to be quadratic in the order parameters. The evolution equations are derived from the free energy variation with respect to the order parameters. The elastic field is determined by superposing the Cerruti solution. Examples of computer simulation are presented. [DOI: 10.1115/1.1469000]

1 Introduction

The thermodynamics and kinetics of bulk ferroelectric materials have been extensively studied ([1]). However, there is little systematic study on the ferroelectric thin films ([2,3]). This paper considers some important issues on the domain dynamics in a ferroelastic epilayer on a paraelastic substrate. Consider a ferroelastic epilayer on a paraelastic substrate. The epilayer is much thinner than the substrate. They are coherent, accommodating the lattice mismatch by elastic deformation. At high temperatures, the epilayer and the substrate surface both have square symmetry, but have different lattice constants. To compensate for the lattice mismatch, the epilayer is under a uniform, biaxial stress state, and the substrate is unstressed. At low temperatures, the epilayer has rectangular symmetry, but the substrate surface still has square symmetry. Because of the broken symmetry, the epilayer now has two variants, equivalent upon a 90-deg rotation (Fig. 1). Within the Ginzburg-Landau framework ([1]), we characterize the ferroelastic state by two order parameters, (p_1, p_2), taken to be the components of a vector lying in the plane of the layer. If the epilayer were unconstrained by the substrate, the two variants would have different spontaneous strain states, equivalent after the 90-deg rotation. This paper considers the epilayer constrained on the substrate. It is sometimes assumed in the literature that the energy ground state is a single-variant epilayer on the substrate. This state is illustrated in Fig. 2(*a*). The stress state in the epilayer is uniform and biaxial, with unequal components in the two directions. The substrate is unstressed. Assuming that the epilayer is of a single variant, Pertsev et al. [2] showed that the constraint of the substrate could alter the Curie temperature and even induce new phases.

However, the epilayer of a single variant on the substrate is not the energy ground state ([3–7]). This is readily understood as follows. In Fig. 2(*b*), the two variants coexist and form domains. To aid the argument, imagine that suitable forces are applied on the domain walls, so that the stress state in the old variant is unchanged, the stress state in the new variant is equivalent to the old one after the 90-deg rotation, and the substrate remains unstressed. Consequently, the state in Fig. 2(*b*) has the same elastic energy as the state in Fig. 2(*a*). Now gradually reduce the forces on the domain walls, and allow the epilayer and the substrate to deform. After the forces are completely removed (Fig. 2(*c*)), the displacements are generally in directions opposite from the applied forces in Fig. 2(*b*). Consequently, after elastic relaxation, the two-variant state in Fig. 2(*c*) has lower elastic energy than the single-variant state in Fig. 2(*a*). That is, when the symmetry is broken, due to the substrate constraint, the single-variant epilayer is no longer the energy ground state. This suggests that Pertsev et al.'s assumption of a single variant is excessively simplistic and questions the validity of their results.

Figure 3 illustrates a domain pattern of a periodic array of alternating variants. The smaller the domain size, the more elastic energy is relaxed. Consequently, elasticity drives domains to refine. On the other hand, variants coexist at the cost of adding the domain wall energy. The smaller the domain size, the longer the collective domain walls. That is, the domain wall energy drives the domain to coarsen. The competition between the elastic energy and the domain wall energy selects an equilibrium domain size, which minimizes the combined energy ([3–14]). It is also expected that the minimization of the combined energy can select an equilibrium domain pattern.

This paper introduces a model within the time-dependent Ginzburg-Landau (TDGL) framework to simulate domain dynamics in the epilayer. The epilayer may have different properties from the bulk, particularly if the epilayer is only a few monolayers thick. It may also be possible that a marginally paraelastic bulk crystal is ferroelastic within a few surface layers. Motivated by these considerations, we will model the epilayer-substrate as a single system. The model parallels that for an epilayer with composition modulation ([12–14]). In the present model, the free energy of the system consists of two parts: the bulk elastic energy and the excess surface energy. The elastic energy density is taken to be quadratic in the strains. The excess surface energy density is expanded into a polynomial of the order parameters, the gradients

Contributed by the Applied Mechanics Division of THE AMERICAN SOCIETY OF MECHANICAL ENGINEERS for publication in the ASME JOURNAL OF APPLIED MECHANICS. Manuscript received by the ASME Applied Mechanics Division, March 15, 2001; final revision, December 22, 2001. Associate Editor: D. A. Kouris. Discussion on the paper should be addressed to the Editor, Prof. Robert M. McMeeking, Department of Mechanical and Environmental Engineering University of California–Santa Barbara, Santa Barbara, CA 93106-5070, and will be accepted until four months after final publication of the paper itself in the ASME JOURNAL OF APPLIED MECHANICS.

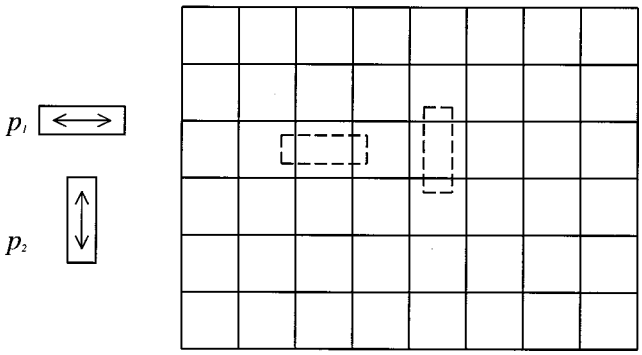

Fig. 1 Broken symmetry and lattice mismatch. The substrate has square symmetry. The epilayer has rectangular symmetry, with two variants.

of the order parameters, and the strains. In this expansion, the surface stress is taken to be quadratic in the order parameters. We derive the evolution equations from the free-energy variation associated with variation in the order parameters, and determine the elastic field by superposing the Cerruti solution. To illustrate the model, we present preliminary results from computer simulations.

The TDGL framework has been applied to bulk ferroelastic crystals ([15–17]). In a bulk ferroelastic single crystal, however, elasticity does not refine domains. In fact, the single-domain crystal is the energy ground state. The bulk elasticity problem lacks an intrinsic length scale. For an infinite, polydomain crystal, the total elastic energy in the crystal is independent of the domain size so long as the domain pattern is self-similar as domains coarsen. In this case, domains coarsen to reduce the domain wall energy. The situation is different if the system is not an infinite single crystal. For a thin ferroelastic film on a substrate ([4–9]), the film thickness provides a length scale. In a polycrystalline crystal, the grain size provides a length scale ([18,19]). In both cases, elasticity does limit the size of the domains. In the model introduced in this paper, the length scale is provided by the introduction of the surface stress, as will be identified in a later section.

2 Free Energy and Kinetic Law

Even for a single crystal, atoms in a few surface layers have different energy from atoms in the bulk. The deposition of the epilayer further changes the energy state. We model the substrate-epilayer system as a bulk solid coupled with a superficial object. The total free energy consists of two parts: the bulk elastic energy and the excess surface energy, written as

$$G=\int WdV+\int \Gamma dA, \tag{1}$$

where W is the elastic energy density, and Γ is the excess surface energy density. The first integral is over the volume of the entire system, and the second integral is over the surface area covered by the epilayer. Following [14], we interpret the surface energy as the excess free energy relative to bulk elastic energy. Thus, Γ includes the effects of the mismatch between the two materials, as well as the presence of the empty space above.

In the rectangular coordinate system, the surface coincides with the (x_1,x_2) plane, and the material occupies the half-space $x_3<0$. Reference the displacement vector in the system u_i from an infinite, unstressed crystal of the same composition as the substrate. The strain tensor ε_{ij} relates to the displacement gradient, namely,

$$\varepsilon_{ij}=\tfrac{1}{2}(u_{i,j}+u_{j,i}). \tag{2}$$

The Latin subscripts run from 1 to 3.

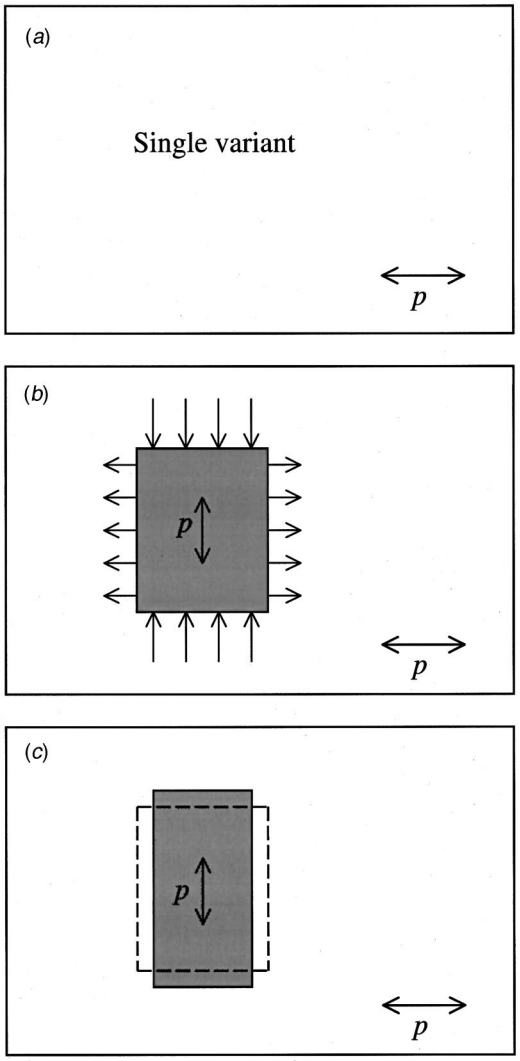

Fig. 2 Schematic illustration of elastic refining; (*a*) a single-variant epilayer, (*b*) a two-variant epilayer with appropriate forces applied around the new domain, (*c*) the external forces removed

We assume that the substrate is elastically isotropic, μ being the shear modulus, and ν Poisson's ratio. The elastic energy density W is quadratic in the strain tensor:

$$W=\mu\left[\varepsilon_{ij}\varepsilon_{ij}+\frac{\nu}{1-2\nu}(\varepsilon_{kk})^2\right]. \tag{3}$$

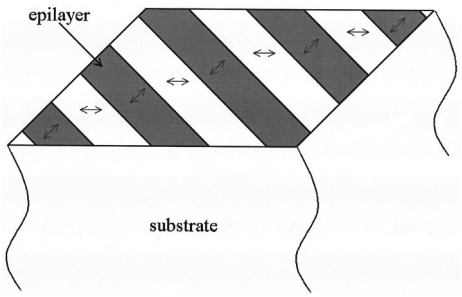

Fig. 3 A domain pattern in the epilayer constrained on the substrate

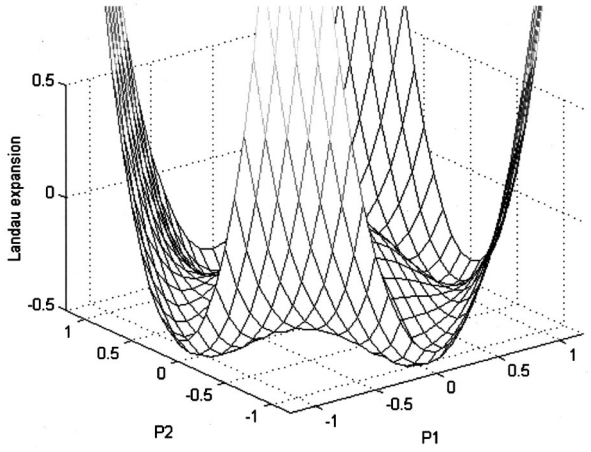

Fig. 4 The Landau expansion as a function of the order parameters. The four wells correspond to spontaneous states.

The stresses σ_{ij} in the bulk are the differential coefficients of the elastic energy density:

$$\delta W = \sigma_{ij}\delta\varepsilon_{ij}. \tag{4}$$

The repeated subscripts imply the summation convention.

We characterize the ferroelastic state of the epilayer by two order parameters, p_1 and p_2, which form the components of a vector lying in the plane of the epilayer. For example, when the layer is also ferroelectric, this vector coincides with the polarization. The excess surface energy density Γ is a function of the order parameters, the gradients of the order parameters, and the strains. Following the Ginzburg-Landau formalism, we expand Γ into a Taylor series to the lowest terms in $p_{\alpha,\beta}$ and $\varepsilon_{\alpha\beta}$:

$$\Gamma = f_L(p_\xi) + f_G(p_{\alpha,\beta}) + f_{\alpha\beta}(p_\xi)\varepsilon_{\alpha\beta}. \tag{5}$$

The Greek letters run from 1 to 2. The physical content of every term in (5) is interpreted as follows.

The first term in (5) is the Landau expansion. We assume that the epilayer has square symmetry in the high-temperature phase. The Landau expansion takes the following form ([15–17]):

$$f_L = a_0 + a_1(p_1^2+p_2^2) + a_{11}(p_1^4+p_2^4) + a_{12}p_1^2p_2^2 + a_{111}(p_1^6+p_2^6) + a_{112}(p_1^4p_2^2+p_1^2p_2^4). \tag{6}$$

Here a_0 is the surface energy density of the epilayer on the substrate when the epilayer is in the paraelastic phase ($p_\alpha=0$) and the substrate is unstrained ($\varepsilon_{\alpha\beta}=0$). The coefficient a_1 is proportional to $T-T_C$, i.e., the temperature difference from critical point, T_C. When $T<T_C$, $a_1<0$, and the function has four wells (Fig. 4). Each well corresponds to an unconstrained ferroelastic variant. There is no reason to regard the coefficients in (6) to be the same as those of bulk materials.

The second term in (5) stands for the gradient energy, which is taken to be quadratic in the gradients of the order parameters ([15–17]):

$$f_G(p_{\alpha,\beta}) = \tfrac{1}{2}g_{11}(p_{1,1}^2+p_{2,2}^2) + g_{12}p_{1,1}p_{2,2} + \tfrac{1}{2}g_{44}(p_{1,2}+p_{2,1})^2 + \tfrac{1}{2}g'_{44}(p_{1,2}-p_{2,1})^2. \tag{7}$$

The g parameters are positive constants. This is a continuum description of the domain wall energy.

The third term in (5) gives the strain dependence. We have only included the linear terms of the strains, neglecting the excess elastic constants of the epilayer relative to the substrate. The latter could also be included as a refinement of the theory. The coefficients $f_{\alpha\beta}$ are the components of the surface stress tensor. The surface stress tensor has been incorporated into the continuum elasticity theory by adding a strain-dependent surface energy to the free energy [10–14]. In this paper, we expand the surface stress $f_{\alpha\beta}$ in terms of the order parameters:

$$\begin{aligned} f_{11} &= f_0 - \tfrac{1}{2}\beta_{11}p_1^2 + \tfrac{1}{2}\beta_{12}p_2^2 \\ f_{22} &= f_0 + \tfrac{1}{2}\beta_{12}p_1^2 - \tfrac{1}{2}\beta_{11}p_2^2 \\ f_{12} &= -\beta_{44}p_1p_2. \end{aligned} \tag{8}$$

Here f_0 is the surface stress when the epilayer is in the paraelastic state. In the ferroelastic state, the surface stress is taken to be quadratic in the order parameters. The surface stress couples the domain pattern in the epilayer to the elastic deformation in the substrate.

The epilayer-substrate is a nonequilibrium thermodynamic system. The system can vary by two means: the elastic displacements and the order parameters. Characterize a virtual change of the system by δu_i and δp_α. The free-energy variation associated with this virtual change is

$$\delta G = \int\left[\frac{\partial f_L}{\partial p_\alpha} - \frac{\partial}{\partial x_\beta}\left(\frac{\partial f_G}{\partial p_{\alpha,\beta}}\right) + \frac{\partial f_{\xi\eta}}{\partial p_\alpha}\varepsilon_{\xi\eta}\right]\delta p_\alpha dA + \int\left[\left(\sigma_{3\alpha} - \frac{\partial f_{\alpha\beta}}{\partial x_\beta}\right)\delta u_\alpha + \sigma_{33}\delta u_3\right]dA + \int \sigma_{ij,j}\delta u_i dV. \tag{9}$$

We assume that elastic relaxation is much faster than domain switching. At a given time the system reaches elastic equilibrium instantaneously. Consequently, the energy variation associated with the elastic displacements vanishes, leading to the familiar equilibrium equations in elasticity:

$$\sigma_{ij,j} = 0, \tag{10}$$

and the boundary conditions:

$$\sigma_{3\alpha} = \frac{\partial f_{\alpha\beta}}{\partial x_\beta}, \quad \sigma_{33} = 0. \tag{11}$$

Associated with the virtual change of the order parameters, the variation of the free energy defines a thermodynamic force, F_α, namely,

$$\int F_\alpha \delta p_\alpha dA = -\delta G. \tag{12}$$

A comparison of (9) and (12) gives that

$$F_\alpha = -\left[\frac{\partial f_L}{\partial p_\alpha} - \frac{\partial}{\partial x_\beta}\left(\frac{\partial f_G}{\partial p_{\alpha,\beta}}\right) + \frac{\partial f_{\xi\eta}}{\partial p_\alpha}\varepsilon_{\xi\eta}\right]. \tag{13}$$

Following [12–14], we adopt a linear kinetic law that the rate of the change of the order parameters is proportional to the driving force, namely,

$$\frac{\partial p_\alpha}{\partial t} = LF_\alpha, \tag{14}$$

where L is the kinetic coefficient. Combining (13) and (14), we obtain the evolution equations for the order parameters:

$$\frac{\partial p_\alpha}{\partial t} = -L\left[\frac{\partial f_L}{\partial p_\alpha} - \frac{\partial}{\partial x_\beta}\left(\frac{\partial f_G}{\partial p_{\alpha,\beta}}\right) + \frac{\partial f_{\xi\eta}}{\partial p_\alpha}\varepsilon_{\xi\eta}\right]. \tag{15}$$

Assuming elastic equilibrium and using the divergence theorem, we obtain the free energy as follows:

$$G = \int [f_L + f_G - \tfrac{1}{2}\sigma_{3\alpha}u_\alpha]dA. \tag{16}$$

The integral extends over the surface area.

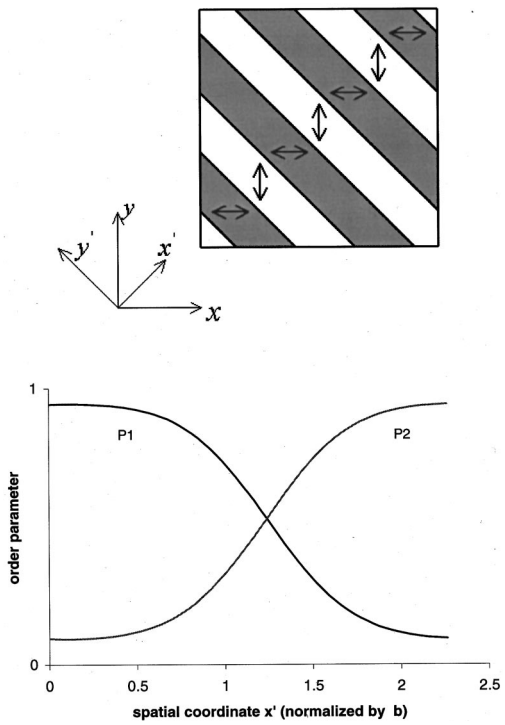

Fig. 5 Domain wall shape. The domain width is on the order of *b*.

3 Dimensionless Equations, Length Scales, and Time Scale

The four wells in the function f_L (Fig. 4) correspond to four states of spontaneous polarization. The value of the spontaneous polarization p_s satisfies

$$a_1+2a_{11}p^2+3a_{111}p^4=0, \tag{17}$$

giving

$$p_s=\left(\frac{-a_1}{a_{11}+\sqrt{a_{11}^2-3a_{111}a_1}}\right)^{1/2}. \tag{18}$$

We use p_s to normalize the order parameters p_1 and p_2.

Introduce dimensionless parameters

$$a'_{11}=\frac{a_{11}p_s^2}{|a_1|},\quad a'_{12}=\frac{a_{12}p_s^2}{|a_1|},\quad a'_{111}=\frac{a_{111}p_s^4}{|a_1|},\quad a'_{112}=\frac{a_{112}p_s^4}{|a_1|}, \tag{19}$$

$$\gamma_1=\frac{g_{12}+g_{44}-g'_{44}}{g_{11}},\quad \gamma_2=\frac{g_{44}+g'_{44}}{g_{11}}. \tag{20}$$

The driving force F_α in (13) contains three terms. The comparison of the terms involving f_L and f_G defines a length scale:

$$b=\sqrt{\frac{g_{11}}{-2a_1}}. \tag{21}$$

This length represents the width of the domain wall in the Ginzburg-Landau framework. We use b to normalize the spatial coordinates. Figure 5 shows the shape of a 90-deg domain wall. In [15], a boundary value problem was solved to obtain the analytical result for the 90-deg domain wall. In our work, the simulation from evolution equations shows similar shape, and the domain wall width is comparable to b.

In (13) a comparison between the gradient energy term and the surface stress term defines another length scale:

$$l=\frac{4\pi\mu g_{11}}{\beta_{11}^2p_s^2}. \tag{22}$$

This length scales the size of an individual domain in an equilibrium pattern. As stated in the Introduction, the equilibrium domain pattern is an outcome of the competition between refining due to elasticity and coarsening due to domain wall energy.

The time scale can be derived from the evolution Eqs. (15), giving

$$\tau=-\frac{1}{2a_1L}. \tag{23}$$

We will report time in the unit of τ.

In terms of the dimensionless quantities introduced above, the evolution equations become

$$\begin{aligned}\frac{\partial p_1}{\partial t}&=p_{1,11}+\gamma_1p_{2,21}+\gamma_2p_{1,22}\\&\quad-\frac{b}{l}\left(-p_1\varepsilon_{11}+\frac{\beta_{12}}{\beta_{11}}p_1\varepsilon_{22}-\frac{2\beta_{44}}{\beta_{11}}p_2\varepsilon_{12}\right)+p_1-2a'_{11}p_1^3\\&\quad-a'_{12}p_1p_2^2-3a'_{111}p_1^5-a'_{112}(2p_1^3p_2^2+p_1p_2^4)\end{aligned} \tag{24}$$

$$\begin{aligned}\frac{\partial p_2}{\partial t}&=p_{2,22}+\gamma_1p_{1,12}+\gamma_2p_{2,11}\\&\quad-\frac{b}{l}\left(\frac{\beta_{12}}{\beta_{11}}p_2\varepsilon_{11}-p_2\varepsilon_{22}-\frac{2\beta_{44}}{\beta_{11}}p_1\varepsilon_{12}\right)+p_2-2a'_{11}p_2^3\\&\quad-a'_{12}p_2p_1^2-3a'_{111}p_2^5-a'_{112}(2p_2^3p_1^2+p_2p_1^4).\end{aligned}$$

In the above the strains have to be determined by solving the elastic field in the semi-infinite solid subject to the following boundary conditions on the surface:

$$\begin{aligned}\sigma_{31}&=-p_1\frac{\partial p_1}{\partial x_1}+\frac{\beta_{12}}{\beta_{11}}p_2\frac{\partial p_2}{\partial x_1}-\frac{\beta_{44}}{\beta_{11}}\left(p_2\frac{\partial p_1}{\partial x_2}+p_1\frac{\partial p_2}{\partial x_2}\right)\\\sigma_{32}&=-p_2\frac{\partial p_2}{\partial x_2}+\frac{\beta_{12}}{\beta_{11}}p_1\frac{\partial p_1}{\partial x_2}-\frac{\beta_{44}}{\beta_{11}}\left(p_2\frac{\partial p_1}{\partial x_1}+p_1\frac{\partial p_2}{\partial x_1}\right)\\\sigma_{33}&=0\end{aligned} \tag{25}$$

where the stress is normalized by $\beta_{11}p_s^2/b$. The elastic field in a half-space due to a tangential point force on the surface is known as the Cerruti field [20]. A superposition gives the needed strain field:

$$\begin{aligned}\varepsilon_{11}&=\int\int\sigma_{31}\left\{-\frac{2(1-3\nu)(x-\xi)}{[(x-\xi)^2+(y-\eta)^2]^{3/2}}\right.\\&\quad\left.-\frac{6\nu(x-\xi)^3}{[(x-\xi)^2+(y-\eta)^2]^{5/2}}\right\}d\xi d\eta\\&\quad+\int\int\sigma_{32}\left\{\frac{2\nu(y-\eta)}{[(x-\xi)^2+(y-\eta)^2]^{3/2}}\right.\\&\quad\left.-\frac{6\nu(y-\eta)(x-\xi)^2}{[(x-\xi)^2+(y-\eta)^2]^{5/2}}\right\}d\xi d\eta\end{aligned}$$

$$\varepsilon_{22}=\int\int \sigma_{31}\left\{\frac{2\nu(x-\xi)}{[(x-\xi)^2+(y-\eta)^2]^{3/2}} - \frac{6\nu(x-\xi)(y-\eta)^2}{[(x-\xi)^2+(y-\eta)^2]^{5/2}}\right\} d\xi d\eta + \int\int \sigma_{32}\left\{-\frac{2(1-3\nu)(y-\eta)}{[(x-\xi)^2+(y-\eta)^2]^{3/2}} - \frac{6\nu(y-\eta)^3}{[(x-\xi)^2+(y-\eta)^2]^{5/2}}\right\} d\xi d\eta$$

$$\varepsilon_{12}=\frac{1}{2}\int\int \sigma_{31}\left\{-\frac{2(1-2\nu)(y-\eta)}{[(x-\xi)^2+(y-\eta)^2]^{3/2}} - \frac{12\nu(x-\xi)^2(y-\eta)}{[(x-\xi)^2+(y-\eta)^2]^{5/2}}\right\} d\xi d\eta + \frac{1}{2}\int\int \sigma_{32}\left\{-\frac{2(1-2\nu)(x-\xi)}{[(x-\xi)^2+(y-\eta)^2]^{3/2}} - \frac{12\nu(x-\xi)(y-\eta)^2}{[(x-\xi)^2+(y-\eta)^2]^{5/2}}\right\} d\xi d\eta. \tag{26}$$

The strains are normalized by $\beta_{11}p_s^2/4\pi\mu b$. The displacements, normalized by $\beta_{11}p_s^2/4\pi\mu$, are

$$u_1=\int\int \sigma_{31}\left\{\frac{2(1-\nu)}{[(x-\xi)^2+(y-\eta)^2]^{1/2}} + \frac{2\nu(x-\xi)^2}{[(x-\xi)^2+(y-\eta)^2]^{3/2}}\right\} d\xi d\eta + \int\int \sigma_{32}\left\{\frac{2\nu(x-\xi)(y-\eta)}{[(x-\xi)^2+(y-\eta)^2]^{3/2}}\right\} d\xi d\eta$$

$$u_2=\int\int \sigma_{31}\left\{\frac{2\nu(x-\xi)(y-\eta)}{[(x-\xi)^2+(y-\eta)^2]^{3/2}}\right\} d\xi d\eta + \int\int \sigma_{32}\left\{\frac{2(1-\nu)}{[(x-\xi)^2+(y-\eta)^2]^{1/2}} + \frac{2\nu(y-\eta)^2}{[(x-\xi)^2+(y-\eta)^2]^{3/2}}\right\} d\xi d\eta. \tag{27}$$

4 Computer Simulation

To illustrate the model, we now present several preliminary computer simulations. Referring to [16,17], we adopt the following parameters:

$$a'_{11}=0.5,\quad a'_{12}=1.74,\quad a'_{111}=0.063,\quad a'_{112}=0.148$$
$$g_{12}/g_{11}=1.1,\quad g_{44}/g_{11}=0.9,\quad g'_{44}/g_{11}=0.1$$
$$b/l=1.0,\quad \beta_{12}/\beta_{11}=0.05,\quad \beta_{44}/\beta_{11}=0.111,\quad \nu=0.3. \tag{28}$$

We have not carried out a comprehensive parametric study.

The evolution equations have both spatial and temporal derivatives. We discretize the infinite surface into an array of squares of size $N\times N$. All fields are assumed to be periodically replicated from one square to another. Each square is the computation unit cell, which is subdivided into grids of spacing Δx. Spatial derivatives are approximated with finite difference. At every time step, the elastic field is calculated by evaluating the double integrals, and the order parameter field is updated by using the Euler method. In our simulation, we use $N=128$, $\Delta x=1.0$, and adaptive time steps. The ratio of two length scales is $b/l=1.0$. The singular integrals in (26) and (27) are evaluated by adopting a technique in the Appendix. Since the double integrals must be calculated for every grid point, the simulation is rather slow. The evolution can also be simulated in reciprocal space ([12–17]), which we will implement for this model in the future.

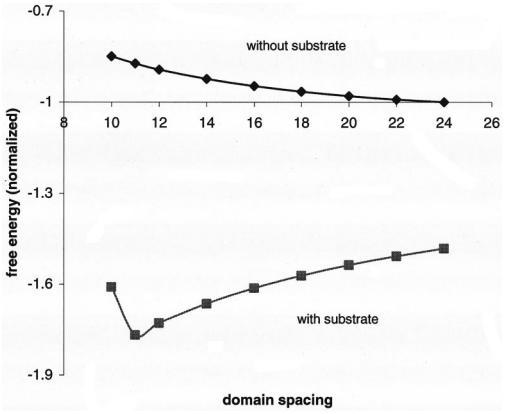

Fig. 6 Free energy versus domain spacing. Without substrate constraint, the energy decreases as the domain size increases. With substrate constraint, the energy reaches a minimum at a specific domain size.

For a given domain pattern, i.e., a prescribed field of the order parameters, the free energy can be computed from Eqs. (16), (25), and (27). In the first simulation, we specify a parallel domain pattern, fix the domain spacing, but allow the domain walls to relax locally. We calculate the free energy as a function of the domain spacing. Figure 6 illustrates the effect of substrate constraint. The domain size in this figure is the width of the domain along (x,y) coordinates of Fig. 5. As discussed in the Introduction, without the substrate, the total free energy of the epilayer decreases with the increase of the domain size, and the single domain has the lowest energy. With the substrate constraint, since the competition of elasticity and domain wall energy selects an equilibrium domain size, a valley exists on the curve of energy versus domain spacing. For the domains smaller than the equilibrium size, the relaxation of the elastic energy cannot accommodate the rapid increase of the domain wall length, so the more domains, the higher the free energy.

Figure 7 compares the domain evolution with substrate and without substrate constraint. Through every grid point we draw a short line segment, representing the magnitude and the direction of the order parameter. The left column shows the result with the substrate, and the right one without substrate. In both cases, we start with the initial condition of a small random perturbation of the order parameter field from zero, corresponding to the paraelastic state. When the layer is constrained, parallel domains form, and the domain size approaches to what has been shown in Fig. 5. When the layer is unconstrained, the domains coarsen, being limited only by the calculating cell size.

5 Summary

This paper presents a formalism to simulate the evolution of domain patterns in ferroelastic epilayers. The surface stress due to the spontaneous strains can be relaxed by the substrate mediated elastic interaction. Free energy is divided into two parts. One is the elastic energy of the semi-infinite substrate, and the other is the excess surface energy, which has the ingredients of the Landau expansion, the gradient energy, and the surface stress. Evolution equations are derived from energy variation. Computer simulation ascertains that the competition of coarsening and refining is responsible for equilibrium domain patterns. The formalism presented in this paper is flexible, and can be used to study other phenomena involving surface phase transition and pattern formation.

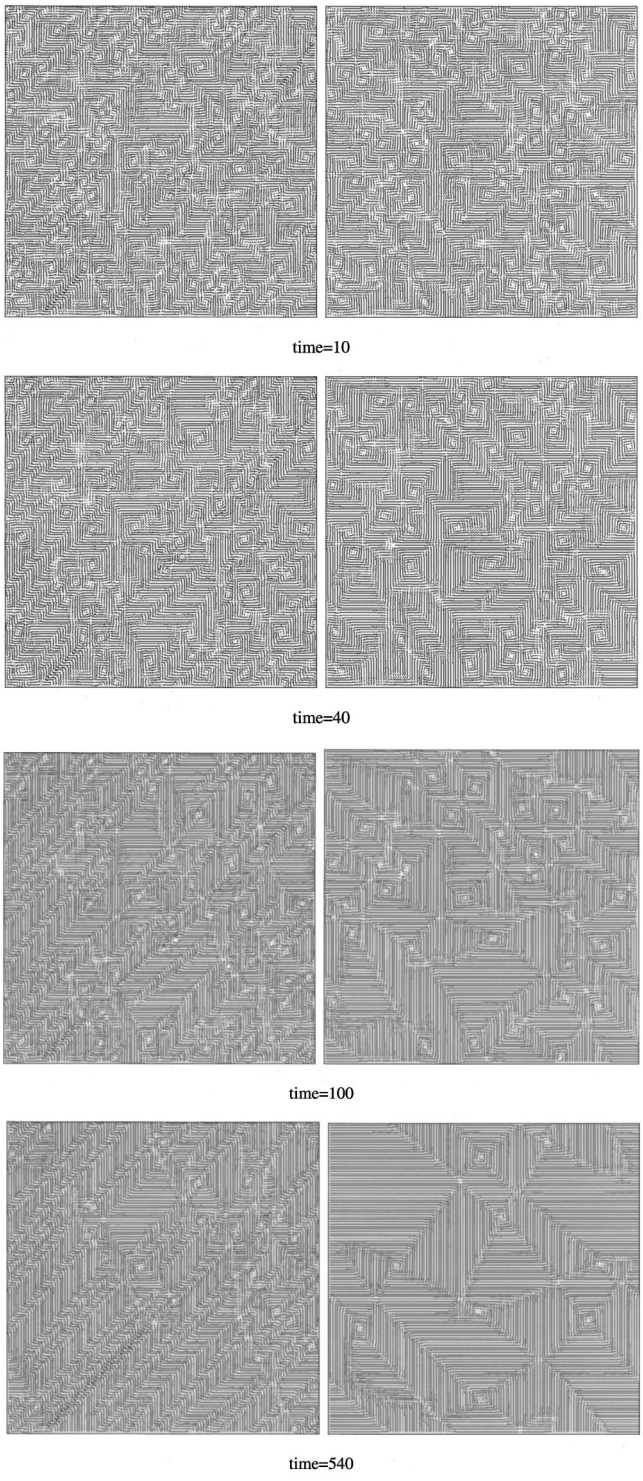

Fig. 7 Comparison of domain evolution in simulations with substrate constraint and without. The left column is the result with substrate, and parallel domains can be seen. The right column is the result without constraint, and the structure keeps coarsening.

Acknowledgments

This work is supported by the National Science Foundation through grant CMS-9820713, and by Princeton University through the Sir Gordon Wu Fellowship for Y. F. G. We would like to thank Dr. Wei Lu for helpful discussions.

Appendix

The integrals (26) and (27) extend over the entire surface. To save computation time, we only extend the integrals to a finite square of size $16b \times 16b$ in our simulation. The integrals are singular when $x=\xi$ and $y=\eta$. Let ε be a small number, say the grid spacing Δx. We treat the singularity as follows:

$$\int_{x-\varepsilon}^{x+\varepsilon}\int_{y-\varepsilon}^{y+\varepsilon}\frac{\sigma_{31}(\xi,\eta)(x-\xi)}{[(x-\xi)^2+(y-\eta)^2]^{3/2}}\,d\xi\,d\eta$$

$$=\int_{x-\varepsilon}^{x+\varepsilon}\int_{y-\varepsilon}^{y+\varepsilon}\frac{[\sigma_{31}(\xi,\eta)-\sigma_{31}(x,y)](x-\xi)}{[(x-\xi)^2+(y-\eta)^2]^{3/2}}\,d\xi\,d\eta$$

$$\approx\int_{x-\varepsilon}^{x+\varepsilon}\int_{y-\varepsilon}^{y+\varepsilon}\frac{\left[\frac{\partial\sigma_{31}}{\partial x}(\xi-x)+\frac{\partial\sigma_{31}}{\partial y}(\eta-y)\right](x-\xi)}{[(x-\xi)^2+(y-\eta)^2]^{3/2}}\,d\xi\,d\eta$$

$$=-\frac{\partial\sigma_{31}}{\partial x}\int_{x-\varepsilon}^{x+\varepsilon}\int_{y-\varepsilon}^{y+\varepsilon}\frac{(x-\xi)^2}{[(x-\xi)^2+(y-\eta)^2]^{3/2}}\,d\xi\,d\eta$$

$$=-\frac{\partial\sigma_{31}}{\partial x}\cdot\varepsilon\cdot\int_{-1}^{1}\int_{-1}^{1}\frac{s^2}{[s^2+t^2]^{3/2}}\,ds\,dt$$

$$=4\ln(\sqrt{2}-1)\,\varepsilon\,\frac{\partial\sigma_{31}}{\partial x}.$$

References

[1] Lines, M. E., and Glass, A. M., 1977, *Principles and Applications of Ferroelectrics and Related Materials*, Clarendon Press, Oxford.
[2] Pertsev, N. A., Zembilgotov, A. G., and Tagantsev, A. K., 1998, "Effect of Mechanical Boundary Conditions on Phase Diagrams of Epitaxial Ferroelectric Thin Films," Phys. Rev. Lett., **80**, pp. 1988–1991.
[3] Suo, Z., 1998, "Stress and Strain in Ferroelectrics," Curr. Opin. Solid State Mater. Sci., **3**, pp. 486–489.
[4] Pompe, W., Gong, X., Suo, Z., and Speck, J. S., 1993, "Elastic Energy Release due to Domain Formation in the Strained Epitaxy of Ferroelectric and Ferroelastic Films," J. Appl. Phys., **74**, pp. 6012–6019.
[5] Speck, J. S., and Pompe, W., 1994, "Domain Configurations due to Multiple Misfit Relaxation Mechanisms in Epitaxial Ferroelastic Thin Films: I Theory," J. Appl. Phys., **76**, pp. 466–476.
[6] Kwak, B. S., and Erbil, A., 1992, "Strain Relaxation by Domain Formation in Epitaxial Ferroelectric Thin Films," Phys. Rev. Lett., **68**, pp. 3733–3736.
[7] Sridhar, N., Rickman, J. M., and Srolovitz, D. J., 1996, "Twinning in Thin Films—I. Elastic Analysis," Acta Mater., **44**, pp. 4085–4096.
[8] Sridhar, N., Rickman, J. M., and Srolovitz, D. J., 1996, "Twinning in Thin Films—II, Equilibrium Microstructures," Acta Mater., **44**, pp. 4097–4113.
[9] Seul, M., and Andelman, D., 1995, "Domain Shapes and Patterns—The Phenomenology of Modulated Phases," Science, **267**, pp. 476–483.
[10] Ibach, H., 1997, "The Role of Surface Stress in Reconstruction, Epitaxial Growth and Stabilization of Mesoscopic Structures," Surf. Sci. Rep., **29**, pp. 193–263.
[11] Alerhand, O. L., Vanderbilt, D., Meade, R. D., and Joannopoulos, J. D., 1988, "Spontaneous Formation of Stress Domains on Crystal Surfaces," Phys. Rev. Lett., **61**, pp. 1973–1976.
[12] Lu, W., and Suo, Z., 1999, "Coarsening, Refining, and Pattern Emergence in Binary Epilayers," Z. Metallkd., **90**, pp. 956–960.
[13] Lu, W., and Suo, Z., 2001, "Dynamics of Nanoscale Pattern Formation of an Epitaxial Monolayer," J. Mech. Phys. Solids, **49**, pp. 1937–1950.
[14] Suo, Z., and Lu, W., 2000, "Composition Modulation and Nanophase Separation in a Binary Epilayer," J. Mech. Phys. Solids, **48**, pp. 211–232.
[15] Cao, W., and Cross, L. E., 1991, "Theory of Tetragonal Twin Structures in Ferroelectric Perovskites With a First-Order Phase Transition," Phys. Rev. B, **44**, pp. 5–12.
[16] Hu, H.-L., and Chen, L.-Q., 1998, "Three-Dimensional Computer Simulation of Ferroelectric Domain Formation," J. Am. Ceram. Soc., **81**, pp. 492–500.
[17] Nambu, S., and Sagala, D. A., 1994, "Domain Formation and Elastic Long-Range Interaction in Ferroelectric Perovkites," Phys. Rev. B, **50**, pp. 5838–5847.
[18] Cao, W. W., and Randall, C. A., 1996, "Grain Size and Domain Size Relations in Bulk Ceramic Ferroelectric Materials," J. Phys. Chem. Solids, **57**, pp. 1499–1505.
[19] Randall, C. A., Kim, N., Kucera, J. P., Cao, W. W., and Shrout, T. R., 1998, "Intrinsic and Extrinsic Size Effects in Fine-Grained Morphotoropic-Phase Boundary Lead Zirconate Titanate Ceramics," J. Am. Ceram. Soc., **81**, pp. 677–688.
[20] Johnson, K. L., 1985, *Contact Mechanics*, Cambridge University Press, Cambridge, UK, p. 69.